Bistatic and Multistatic Radar Systems

Pavel BEZOUŠEK[1], *Vladimír SCHEJBAL*[2]

[1] Faculty of Electrical Engineering and Informatics, University of Pardubice, Studentská 95, 532 10 Pardubice, Czech Rep.
[2] Jan Perner Faculty of Transport, University of Pardubice, Studentská 95, 532 10 Pardubice, Czech Republic

pavel.bezousek@upce.cz, vladimir.schejbal@upce.cz

Abstract. *Radar systems, based on bistatic radar concept attracted a substantial attention in the recent years. Passive coherent location systems using "transmitters of opportunity" like radio or TV broadcasters, GSM base stations, satellite communication and GNSS signals proved their potential in detection and tracking moving targets over a significant area. In this paper the multistatic location system with non-cooperative transmitters is described and various aspects of signal processing and signal parameters are discussed.*

Keywords

Radar, bistatic, multistatic, coherent, positioning, signal processing.

1. Introduction

The passive radar systems, used for target detection, positioning and tracking exploiting on board pulsed emitters in the 0.8 to 18 GHz band, have a long tradition in the Czech Republic [1], [2]. In recent years, an extended growth of activities in the area of radar systems, based on the concept of the bistatic radar is reported from many research centers and universities. In the bistatic radar, unlike as in the monostatic radar, the transmitter and the receiver are separated by a distance, comparable to the target-to-receiver range [3], [4]. The bistatic radar has a long tradition; the first applications are reported since the pre-war (World War II) period [4]. After the War the concept of the monostatic radar prevailed due to easier synchronization, less problems with transmitter/receiver coherence and better exploitation of the transmitted power. Nevertheless time after time some applications of the bistatic radar concept were reported. The last revival of this idea was certainly evoked by easily accessible powerful digital technology and by a dense coverage of the Earth by a wide variety of electromagnetic sources. The Passive Coherent Location (PCL) systems [9] are based on exploitation of various transmitters "of opportunity" like FM radio, analogue or digital TV broadcasting, GSM base stations, etc. The transmitters cover the monitored area with signals and the PCL system receiver collects the direct signals and signals scattered by surrounding objects. Comparing the direct and the scattered signals it is possible to find positions and velocities of these scattering objects. For implementation of such radar only a simple receiver is needed and all the burden is transferred to the digital signal processing. No wonder that a number of reports on experimental works has been published in recent years, [6], [13]-[17] approving vitality of this idea. Many new signal and data processing methods have been elaborated and proved, curing the weak points of the system, mainly the large signal dynamics and emitters "of opportunity" signals deficiencies.

Nevertheless, it should be recognized that the concept of the "transmitters of opportunity" has limits in quality, reliability and integrity. Also its application in safeguard systems is disputable. But this concept could easily be modified adding the own transmitter(s) with needed characteristics. That is why we decline from the commonly used term PCL in this contribution substituting it by the title Coherent Multistatic Systems.

2. Principles

2.1 Description of Coherent Multistatic Systems

A Coherent Multistatic System consists generally of several transmitters and several receivers located separately at large distances. The transmitters are supposed to cover all the monitored area with their transmitted signals. No synchronization between individual transmitters or transmitters and receivers is required, but exact positions of both transmitters and receivers are needed. That is non-cooperative transmitters are anticipated in our survey. We assume each receiver receives a direct path signal from the transmitter and signals scattered by static terrestrial objects (clutter) and by moving objects like airplane or vehicle (useful signals). Each pair of a transmitter and a receiver acts as a bistatic radar. The bistatic geometry is shown in Fig. 1.

The bistatic radar in this configuration can evaluate the bistatic range $R_B = R_T + R_R$ from the time difference of arrival (TDOA) between the scattered and the direct path. All possible target positions with the identical bistatic range R_B are situated along the ellipse with foci in the receiver and transmitter positions. Moreover as we assume the coherent operation of the radar, a Doppler frequency shift f_D could also be assessed. In our case of bistatic radar, the Doppler shift corresponds to the arithmetic sum of the velocity components v_T and v_R (bistatic velocity) along the R_T and R_R radii. While the range resolution ΔR depends mainly on the effective signal bandwidth B, the resolution in the Doppler frequency Δf is roughly equal to the reciprocal of integration time T_i:

$$\Delta R = c/(2B)\,,\ \Delta f = 1/T_i\,. \tag{1}$$

If only the bistatic range and the Doppler frequency shift are evaluated from signal processing of one transmitter – receiver pair, minimally two transmitters or two receivers are needed to find the target horizontal position at intersection of the ellipses. But in the frequent case when many targets are present it leads to severe problems with elimination of many false targets. Each target generates one ellipse for one transmitter – receiver (T/R) pair. If N of T/R pairs are used and M targets are present then we have $N.(N-1)M^2$ intersections, from which only M correspond to positions of real targets. For instance in a very modest case of $N = 3$, $M = 5$, we will have 145 false target positions and only 5 positions corresponding to the real targets. As we may see it would be very plausible to determine the target position directly from one T/R pair measurement to decrease processing complexity in the target association phase. Fortunately one of the first steps in the signal processing is forming a deep null in the direction of the transmitter to suppress the direct signal. Such an antenna array also makes possible a measurement of direction of signal arrival (DOA) (or the bistatic angle Θ_R). Therefore, in this contribution, receivers with some bearing measurement capability are assumed.

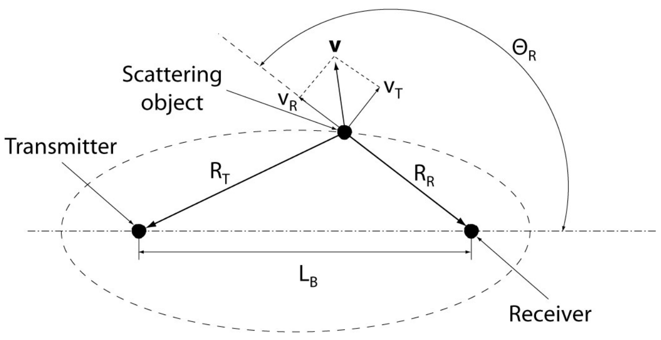

Fig. 1. Bistatic radar geometry: L_B is the length of the bistatic radar base, R_T, R_R are the transmitter - object and object - receiver ranges, Θ_R is the DOA angle of the received signal, scattered by the object.

2.2 The Bistatic Radar Equation

The radar equation for the monostatic radar is a resource of many useful relations such as the Range equation [3]. In the case of bistatic radars the radar equation is relatively simply to derive [4] but its application is much more complicated. The bistatic radar equation holds:

$$P_R = P_T G_T G_R \frac{f_T^2(\Phi,\Theta) f_R^2(\Phi,\Theta)\lambda^2\sigma_B}{(4\pi)^3 R_T^2 R_R^2 L_{TR}}\,. \tag{2}$$

where P_T, P_R are the transmitted and received powers, G_T, G_R are the transmitter and receiver antennas gains, f_T, f_R are the transmitter and receiver voltage antennas characteristics, λ is the wavelength of the transmitted signal, σ_B is the target effective bistatic cross-section, L_{TR} is the loss on the transmitter - receiver path.

Two simplifications in (2) could be readily done – the first: the transmitter antennas are usually omnidirectional, so that the antenna characteristics f_T could be let out of the equation (2) and the second: the product $P_T G_T$ could be substituted by the Effective Radiated Power ERP.

There are several competitive signals reducing the maximum range and complicating the signal processing. They are: the direct signal, correlated reflections of terrain objects (clutter), non-correlated signals transmitted by other sources at the same frequency (electromagnetic noise) and the thermal noise. Now we will demonstrate the signal dynamics on a particular example. Let us assume the following parameters: ERP = 10 kW, G_R= 3 dB, R_R=50 km, R_T = 80 km, T_S = 600 K (effective noise temperature), B = 100 kHz (signal bandwidth), L_B = 100 km, σ_B = 10 m^2, σ_C = 10 000 m^2 – 100 000 m^2 (clutter), λ = 3 m, f_R = 1, L_{TR} = 1. The results are shown in Tab. 1.

Signal	Power at the receiver	Relative level
Thermal noise	-121,0 dBm	+8,8 dB
Direct signal	-37,7 dBm	+92,1 dB
Electromag. noise	-90,0 dBm (see [9])	+39,8 dB
Clutter	- 99,8 dBm	+30 – 40 dB
Received signal	-129,8 dBm	0,0 dB

Tab. 1.

We may see that the level of the received direct signal is approximately by 90 dB higher than that of the useful received signal, scattered by a moving object. The reasonable quality of the moving target detection requires the level of unwanted signal to be about 15 dB under the desired signal level. Direct signal should then be suppressed by about 100 – 110 dB. The final Doppler signal processing will of course restrain all the signal components with zero Doppler shifts including the direct signal, but the amount of this suppression is limited by finite frequency sidelobe level of the ambiguity function of the transmitter signal used. So there is a strong demand to cancel the direct signal in the preceding processing steps as much as possible. Usually this is suggested to be done by means of the following procedures:

- adaptive antenna nulling in the direction of the receiver,
- the direct signal subtraction from the complete received signal (in this case the direct signal is received

by another directional antenna and cleaned of the scattered signals by an equalization algorithm),

- adaptive filtering of the received signal.

The direct signal cancellation using the receiver antenna leads to limitation of the area of surveillance in the direction of the transmitter. It could be overcome using more than two non-in-line transmitters (or receivers).

The non-correlated electromagnetic noise and thermal noise could be treated in a common way. This aggregate noise level is about 40 dB over the level of the useful signal. To achieve reasonable false alarm rate we need signal to noise ratio (min.) of about 13 dB. This calls for S/N enhancement of about 50 dB. It could be performed by integration, provided the integration time will be at least $T_i = 1$ s. The integration time is limited by the tracked object acceleration. The realistic estimation of the maximum integration time is (see [9]):

$$T_{i\max} \leq \sqrt{\frac{\lambda}{a}} \tag{3}$$

where a is the object acceleration along the bistatic path ($R_T + R_R$). Usually $a < 1$ ms^{-1} and $\lambda \sim 1$ m, then the integration time of about 1 s is available.

The clutter generated by fix scatterers was modeled in our example by a single scatterer of high bistatic RCS. Relatively little was published on the bistatic clutter magnitude and its statistics. It is supposed the average scattered power could be expressed by the resolution cell area, the two bistatic angles and some quantitative parameters of the illuminated surface as in the case of monostatic radars. It is clear that, if the resolution cell area decreases, the average scattered power will also decrease and the probability of a high RCS scatterer occurrence in the resolution cell will fall down. As we can see the clutter should be suppressed by about 50- 60 dB in our example. This could be performed mainly by the Doppler processing. Unfortunately its effectiveness is limited by the frequency domain sidelobe level of the ambiguity function of the used signal as was claimed above.

2.3 Bistatic Radar Cross Section (RCS)

The bistatic equivalence theorem [3], [4] states that the bistatic RCS of a sufficiently smooth, perfectly conducting target is equal to the monostatic RCS at the bisector of the bistatic angle. Sufficiently smooth targets are typically spheres, elliptic cylinders, cones, and ogives. The differences could be expected, and therefore the results should be used with care. They are created by various reasons such as changes in relative phase between discrete scattering centers, changes in radiation from discrete scattering centers and changes of centers - new centers appear or previous centers disappear. Usually, a bistatic RCS is lower than the monostatic RCS for complex targets. However, some target aspect angles can generate a low monostatic RCS and a high bistatic specular RCS at specific bistatic angles (especially for targets designed for low monostatic RCS over a range of aspect angles) and shadowing that sometimes occur in a monostatic geometry is not present in a bistatic geometry.

A limiting case of the bistatic geometry occurs when the target is on the transmitter-receiver baseline. A substantial enhancement in scattering can be created, even for stealth targets, due to the forward scatter phenomenon. This is thanks to Babinet's principle. In this case, a perfectly absorbing target will generate the same forward scatter as a target shaped hole in a perfectly conducting screen. The forward scatter RCS σ_F is approximately

$$\sigma_f = 4\pi A^2 / \lambda \tag{4}$$

where A is the target projected area and λ is the wavelength.

The above results can be demonstrated by Fig. 2. That gives an idea about the variations of $D = 10 \log \sigma/kal^2$ for the perfectly conducting infinitely long cylinder with radius of $a = 0.5$ m, where σ is the bistatic RCS per unit length calculated by separation of variables, kal^2 is the monostatic RCS of the perfectly conducting cylinder with the length of l, $k = 2\pi/\lambda$, E or H indicates that incident electric or magnetic field is parallel to the cylinder axis and the number indicates the bistatic angle (e.g. RCS E 90 indicates that incident electric field is parallel to the cylinder axis and bistatic angle is 90 degrees).

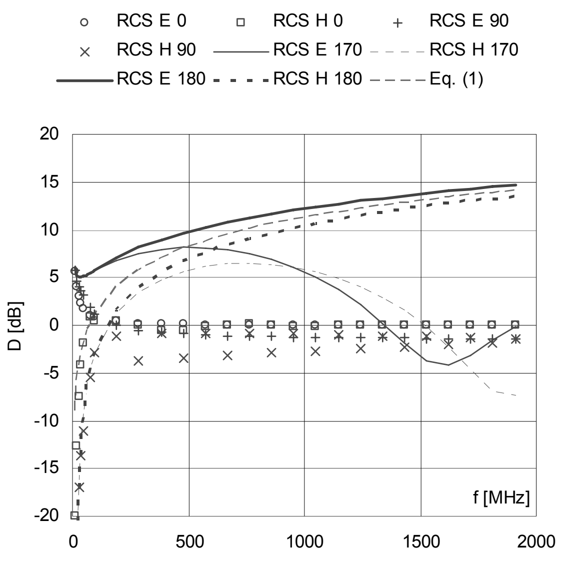

Fig. 2. Variations of $D = 10 \log \sigma/kal^2$ for the perfectly conducting cylinder with radius of $a = 0.5$ m (RCS E 90 indicates that incident electric field is parallel to the cylinder axis and bistatic angle is 90 degrees etc.).

It can be clearly seen that the bistatic RCS for bistatic angle of 90 degrees (i.e. RCS E 90 and RCS H 90) are slightly lower than the monostatic RCS (i.e. RCS E 0 and RCS H 0). The forward scattering (i.e. RCS E 180 and RCS H 180) is much bigger than the monostatic RCS. For lower frequencies, the bistatic RCS for bistatic angles near by 180 degrees (such as RCS E 170 and RCS H 170) is bigger. That is due to the fact that the null-to-null beam width of the scattering is approximately

$$\theta_0 \approx 57\lambda / d \ \text{[deg]} \tag{5}$$

where d is the target linear dimension. That means that the forward scattering is bigger for higher frequencies according to (1) but the null-to-null beam width is very narrow. Moreover, if the radar wavelength is roughly twice the size of the target, a half-wave resonance effect can still generate a significant return. Generally, radar absorbing materials, which use materials such as graphite-ferrite microspheres, could be less efficient for lower frequencies.

Papers [5] and [8] present the results of bistatic RCS calculations and measurements for some real objects like aircrafts in the 160, 390, 850 and 3000 MHz frequency bands. The experimental data demonstrated that the RCS at forward scattering is bigger then the monostatic case by 30-40 dB depending on frequency band.

Fig. 3 shows forward scatter RCS σ_F according to (1) and θ_0 according to (2) for $A = 20$ m^2 and $d = 20$ m. That could be considered as typical values for aircrafts. The RCS σ_F calculation (F-117A [8]) and measurements (Mi-2 helicopter [8], TU 134 and Orion [5]) are shown for comparison. It can be concluded that frequencies around VHF/UHF could be optimum for forward scatter [4].

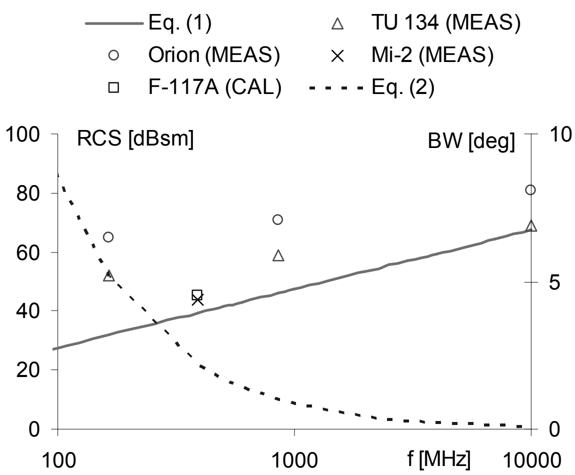

Fig. 3. Calculated forward scatter RCS σ_F and θ_0 for $A = 20$ m^2 and $d = 20$ m. RCS σ_F calculation (F-117A [8]) and measurements (Mi-2 helicopter [8], TU 134 and Orion [5]).

2.4 Bistatic Clutter

Bistatic clutter could be more variable than the monostatic clutter, as more variables associated with the geometry exist. The clutter RCS σ_c is the product of the bistatic backscatter coefficient σ_b and the clutter resolution cell area A_c. Both parameters depend on geometry (with the maximum value of σ_b at specular angles). Experimental data and models for bistatic clutter are limited [3], [4], [6] and [7]. Values for horizontal and vertical polarization showed no significant differences. Mostly, both monostatic and bistatic data exhibited nearly log-normal amplitude distributions.

3. Signal Processing

The signal processing in Coherent Multistatic Systems could be described using a block diagram in the Fig. 4. In the input part the received signal in each antenna element is downconverted, separated according to the transmitter's bands and converted to digital. Then adaptive beamforming systems at each transmitter band (such as described in [21], which use the genetic algorithm) create minimally two beams for each transmitter (see Fig. 5): the first one with a deep null in the direction of transmitter to suppress the direct path signal (the target channel) and the second one with its maximum in the transmitter direction (the reference channel). In the earlier implementations, only two directional antennas were frequently used - one of them headed to the transmitter and the other to the observed object.

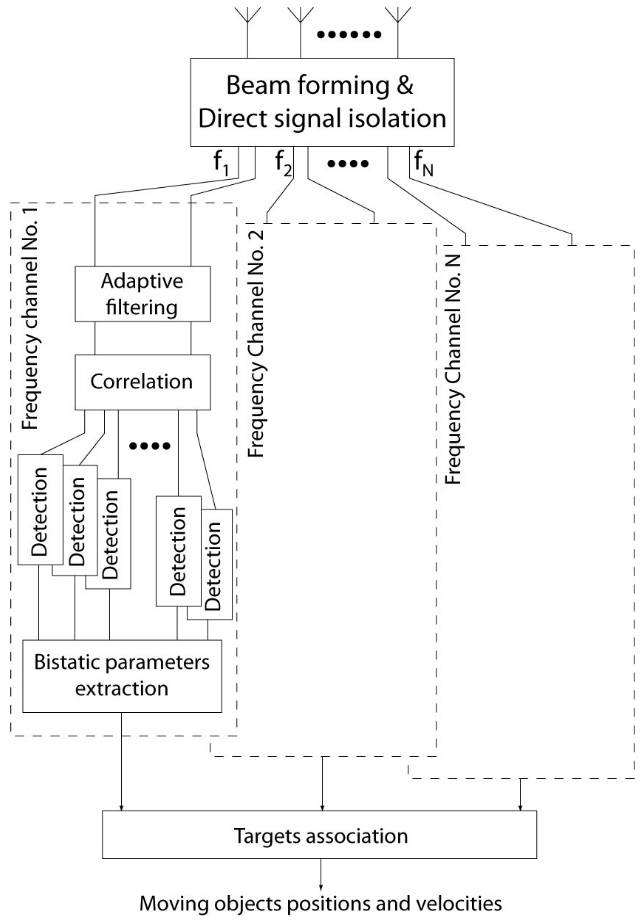

Fig. 4. A basic block diagram of the signal processing in CMS.

The amount of the direct signal suppression in the target channel at the output of this stage is roughly equal to the direct signal power overlap over the joint power of clutter, noise and the useful signal. It is of about 50 dB in our demonstration example.

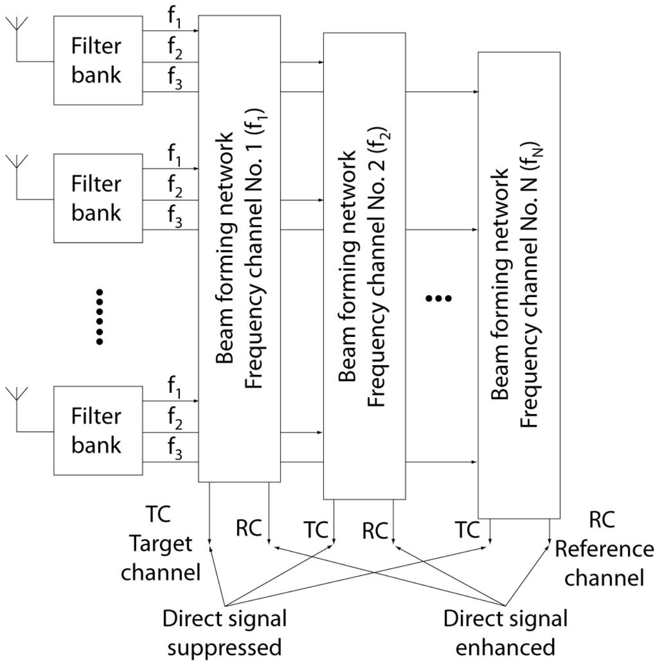

Fig. 5. Antenna subsystem - the direct and scattered signals separation.

In the further processing stage the direct signal filtration and subtraction of the rest of the direct signal from the target channel take place (Fig. 6). First the direct signal in the reference channel should be cleaned out of the accompanying highly correlated clutter, formed by reflections from stationary objects. This is a standard procedure, called equalization. In communication systems, a number of blind equalization methods is used [10]. But in our case (compared to the equalization in communication) also a correct time shift of the direct signal should be evaluated. The next step is the subtraction of the direct signal from the target channel. The best amplitude, phase and time-shifts should be found to minimize the content of the direct signal in the target channel. Efficient algorithms of the procedure have been published, suited particularly for this case [11], [4], [13]. The estimated suppression of the direct signal in this stage is about 40 – 50 dB. In the next stage correlation of the signal in the Target Channel with a direct signal from the Reference Channel is performed.

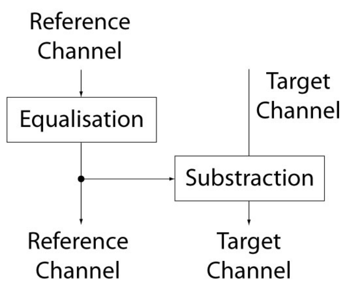

Fig. 6. An adaptive filtration stage.

The circuit correlates the signal from the target channel, shifted in frequency by selected frequency shifts f_{di} with a copy of the transmitted signal and acts like a bank of matched filters. As a result an estimate of the cross-ambiguity function between both channels is acquired:

$$CAF(\tau, f) = \int_{-\infty}^{+\infty} s_T(t) s_R^*(t+\tau) \exp(j\omega t) dt \tag{6}$$

where $s_T(t)$, $s_R(t)$ are the target and reference channel signals, $\omega=2\pi f$ is a particular frequency shift.

In practice the correlation is better to carry on in the frequency domain. We may assume that the signal in the target channel consists of a desired signal, scattered by a moving object, of the residual direct signal, of clutter and of noise:

$$\begin{aligned} s_T(t) &= a_0 . s_1(t - t_D) . \exp(-j\omega_d t) + \\ &+ \sum_i a_i . s_1(t - t_{Di}) + n(t) \end{aligned} \tag{7}$$

Then:

$$\begin{aligned} CAF(\tau, f) &= a_0 \int_{-\infty}^{+\infty} s_A(t - t_D) s_A^*(t+\tau) \exp[j(\omega - \omega_d)t] dt + \\ &+ \sum_i a_i \int_{-\infty}^{+\infty} s_A(t - t_{Di}) s_A^*(t+\tau) \exp[j\omega t] dt + \\ &+ \int_{-\infty}^{+\infty} n(t) s_A^*(t+\tau) \exp[j\omega t] dt = \\ &= a_0 AF(\tau - t_D, f - f_D) + \sum_i a_i AF(\tau - t_{Di}, f) + \\ &+ CAF_N(\tau, f) \end{aligned} \tag{8}$$

where $s_A(t)$, $n(t)$ are the transmitted signal and noise, a_0, a_1 are the complex amplitude of a moving object scattered signal and of the remaining direct signal, a_i, $i>1$ are the complex amplitudes of signals, scattered by stationary objects, t_D, t_{Di}, $i>1$ are the time delays of scattered signals, comprising bistatic time delays and processing times, AF is the ambiguity function of the transmitted signal, CAF_N is the noise/transmitted signal cross-ambiguity function.

We may see, that the right hand side of (8) consists of a sum of scaled and time and frequency shifted ambiguity functions $AF(\tau,f)$ of the transmitted signal and of a noise/transmitted signal cross-ambiguity function $CAF_N(\tau,f)$. The first term corresponds to the moving object with the Doppler frequency shift f_D, the following sum represents the direct signal and signals scattered by stationary objects. Further we will concern only with the absolute value of the CAFs and AFs. The noise term (its absolute value) has no significant maxima and its mean level could be effectively minimized using sufficiently long integration period T_i. The absolute value of the ambiguity function of the transmitted signal has dominant maxima and a complicated structure of side lobes.

The main task is to find maxima of the absolute value of the cross-ambiguity function $|CAF(\tau, f)|$ for nonzero frequency shifts. Positions of these maxima in the (τ, f) plane are delays $\{\tau_n\}$ and Doppler frequency shifts $\{f_{dn}\}$, corresponding to the wanted bistatic ranges $\{R_{Bn}\}$ and velocities $\{v_{Bn}\}$ of moving objects. Unfortunately the ambiguity functions of transmitters of opportunity have various imperfections (from the point of view of radar function), which highly complicate the further processing.

Examples of ambiguity functions of various transmitters were studied widely [18]. The width of the main peak determines the ultimate bistatic range and velocity resolution. The level of sidelobes limits the maximum suppression of the direct signal residue and clutter and hence system dynamics, which affects the system maximum range. Many studies and analysis of all possible transmitters of opportunity as well as practical experiments with many of them [13] - [17] have been undertaken. The main characteristics of these transmitters are summarized in Tab. 2.

Transmitter	Typ. ERP [kW]	Level [dBm/m^2]	Range resolution [km]	Peak sidelobe level	
				Range [dB]	Doppler [dB]
FM analogue radio	50		1.8 – 16.5*	-12.0 -27.0*	-26 –46.5
Analogue TV	100		9.6** – 15.6	-0.2	-9.1
DAB	10		1.5	-11.7	-38.0
DTV	10		0.044[1]	-18.5	-34.6
GPS		-135	0.030[2]		
GSM 900 MHz		- 80***	1.8	-9.3	-46.7

Tab. 2. Transmitters of Opportunity Signal Characteristics (After [17][18][19]) :
* depending on program broadcasted,
** using only the chrominance subcarrier,
*** at the range 10 km off the base station,
[1] computed from parameters published in [17],
[2] computed from parameters published in [20].

It was approved by several authors that the actual bandwidth of the FM radio signal fluctuates according to the contents of the program broadcasted. The fluctuations are very pronounced namely in the case of an analogue FM transmitter broadcasting speech. Better results are obtained with Digital Audio Broadcast, which has a stable full width bandwidth due to channel coding and interleaving of the digital signal. On the other hand, another problem arises with DAB due to a considerable lower ERP used, compared to analogue transmitters. Analogue TV transmitters feature a significant ERP and good area coverage, but its ambiguity function has very poor characteristics from the radar's point of view. Its effective bandwidth is only about 20 kHz, leading to range resolution of 15 km. Due to a very strong correlation between individual lines (of the TV image), very high sidelobe levels are achieved both in range and in frequency. Nevertheless, the successful application of analogue TV broadcaster in the PCL system has been reported ([14]). The digital TV broadcasting attains better performance. The signal spans all the 6.7 MHz (even 8 MHz in Europe) due to image compression (all redundancies are substantially suppressed). The image signal is practically non-correlated (noise-like), but there are still some deterministic components in the signal, generating high ambiguities (very high sidelobe levels). Fortunately the structure of those components is well known and stability of timing is pretty high so the ambiguities could be extracted using proper time keying of the processing procedures ([17]). Another problem arises from the fact that the near range sidelobes of the ambiguity function are unfavorably high but they rapidly decrease with the increasing distance.

Relatively little has been reported on the application of GPS or other navigation satellite signals. With such a system, a very good range resolution is anticipated but great problems could arise from the fact that all satellites use the same frequency and that the satellites move with velocities of about 3000 m/s.

A GSM base station signal is relatively weak comparing to the radio and TV transmitters so only a short range could be achieved. The GSM signal also contains deterministic and pseudo periodical components, creating high sidelobes. Unfortunately too little authors devoted their effort to practical implementations of the system, based on GSM transmitters.

After the matched filtration the signal detector using CFAR (Constant False Alarm Rate) algorithms are applied. Some authors indicate application of CA CFAR with reasonable results. This kind of CFAR could be well adequate only for smooth and well distributed clutter. In our case the statistics of the remaining scattered signals (suppression of about 50 dB) and of the direct signal (suppression about 120 dB) is highly irregular, so a further study and implementations in this area are needed.

In the systems with a bistatic angle measurement capability, each transmitter/receiver pair may find targets positions independently on the other T/R pairs. A sophisticated application of Kalman tracking even in the case of a very poor range and angle resolution leads to satisfactory results as was demonstrated in [14]. Association of tracks of individual T/R pairs is then a standard tracking problem.

On the other hand the signal association is a very difficult task in a system, where the target position is not estimated at the bistatic radar level. Then the problem of many false target positions (ghost targets) arises. In the last years, the Probability Hypothesis Density (PHD) based particle filter has been successfully used to solve this difficult problem (see [20] for instance).

4. Conclusion

In this paper, the systems based on the concept of bistatic radars and using non-cooperative transmitters are described. These systems need only a simple RF hardware but a large amount of signal processing. Number of authors has demonstrated creative solutions of particular problems, but there are still many objectives to solve to build an independent system for practical use. The challenging problems are: angle measurement, target detection and association, application of GNSS and DTV signals. The attention should also be paid to systems using an intended transmitter. It could be used for safeguarding systems in a limited area of several km, where the transmitters of opportunity do not afford sufficient level of integrity and safety.

Acknowledgements

The paper is supported by the Czech Ministry of Transportation research grant No. CG743-037-520 and by the Czech National Institutional Research "Theory of Transport System" No. MSM 0021627505.

References

[1] SCHEJBAL, V. et al. Czech radar technology. *IEEE Transaction on Aerospace and Electronics Systems*, 1994, vol. 30, no. 1, p. 2 – 17.

[2] BEZOUSEK, P., SCHEJBAL, V. Radar technology in the Czech Republic. *IEEE Aerospace and Electronic Systems Magazine*, 2004, vol. 19, no. 8, p. 27-34.

[3] SKOLNIK, M. I. *Radar Handbook.* 2nd ed. Boston, Mass: McGraw-Hill, 1990.

[4] GRIFFITHS, H. D. *Bistatic and Multistatic Radar* [online]. 2003 [cit. 2008-06-27]. Available: <www2.theiet.org/oncomms/pn/radar/Griffiths%20Shrivenham.pdf>

[5] CHESNOKOV, Y. S., KRUTIKOV, M. V. Bistatic RCS of aircrafts at the forward scattering. In *CIE International Conference of Radar Proc,* 1996, p. 156 – 159.

[6] SLEZAK, L., KVASNICKA, M., PELANT, M., VAVRA, J., PLSEK R. *Passive Coherent Location System: Simulation and Evaluation.* [online], Available: <http://www.erabeyondradar.com/documents/white-papers/Surveillance/pcl-system-simulation-and-evaluation.pdf>

[7] GIERULL, C. H. *Bistatic Synthetic Aperture Radar.* [online]. Available: <http://pubs.drdc.gc.ca/PDFS/unc34/p523308.pdf>

[8] BLYAKHMAN, .B., RUNOVA, I. A. Forward scattering radiolocation bistatic RCS and target detection. In *IEEE Radar Conference,* Waltham (MA), 1999, p. 203 – 208.

[9] GRIFFITHS, H. D., BAKER, C. J. Passive coherent location radar systems. Part I: Performance prediction. *IEE Proc. Radar, Sonar Navigation*, 2005, vol. 152, no. 3, p. 153 – 159.

[10] PROAKIS, J. G. *Digital Communication*. New York: Mc.Graw-Hill, 1996.

[11] GUNER, A., TEMPLE, M.A., CLAYPOO, JR., R.L. Direct path filtering of DAB waveform PCL receiver target channel. *Electronic Letters*, 2003, vol. 39, no. 1, p. 118 – 119

[12] TAN, D.K.P., SUN, H., LU, Y., LESTURGIE, M., CHAN, H. L. Passive radar using Global System for Mobile communication signal: theory, implementation and measurements. *IEE Proc. of Radar and Sonar Navig.*, 2005, vol. 152, no. 3, p. 116-123.

[13] HOWLAND, P. E., MAKSIMJUK, D., REITSMA, G. FM radio-based bistatic radar. *IEE Proc. of Radar and Sonar Navig.*, 2005, vol. 152, no. 3, p. 1007-1016.

[14] HOWLAND, P. E. Target tracking using TV-based bistatic radar. *IEE Proc. of Radar and Sonar Navig.,* 1999, vol. 146, no. 3, p. 166-174.

[15] POULIN, D. Passive detection using digital broadcasters (DAB, DVB) with COFDM modulation. *IEE Proc. of Radar and Sonar Navig.*, 2005, vol. 152, no. 3, p. 143-152.

[16] SUN, H., TAN, D.K.P., LU, Y. Design and implementation of GSM based passive radar. In *IEEE Conf. Radar*, 2003, p. 418-422.

[17] SAINI, R., CHERNIAKOV, M. DTV signal ambiguity function analysis for radar application. *IEE Proc. of Radar and Sonar Navig.*, 2005, vol. 152, no. 3, p. 133-142.

[18] GRIFFITHS, H. D. et al. Measurement and analysis of ambiguity functions of off-air signals for PCL. *Electronic Letters*, 2003, vol. 39, no. 13, p. 1005 – 1007.

[19] HE, X., CHERNIAKOV, M., ZENG, T. Signal detectability in SS-BSAR with GNSS non-cooperative transmitter. *IEE Proc. of Radar and Sonar Navig.*, 2005, vol. 152, no. 3, p. 124-132.

[20] TOBIAS, M., LANTERMANN, A. D. Probability hypothesis density-based multitarget tracking with bistatic range and Doppler observations. *IEE Proc. of Radar and Sonar Navig.,* 2005, vol. 152, no. 3, p. 195-205.

[21] HAUPT, R. L. Phase-only adaptive nulling with a genetic algorithm. *IEEE Transactions on Antennas and Propagation,* 1997, vol. 45, no. 6, p. 1009 – 1015.

About Authors...

Pavel BEZOUŠEK was born in Ostrava, Czechoslovakia in 1943. He received his MS degree from the Czech Technical University in Prague in 1966 and his PhD degree from the same university in 1980. He was with the Radio Research Institute of the Tesla Pardubice from 1966 till 1994, where he was engaged in microwave circuits and systems design. Since then he is with the University of Pardubice, now at the Faculty of Electrical Engineering and Informatics. Presently he is engaged in radar systems design.

Vladimír SCHEJBAL was born in 1941. He received his MS from the Czech Technical University in Prague in 1970 and his PhD from the Slovak Academy of Sciences in Bratislava in 1980. He was with the Radio Research Institute of Tesla Pardubice from 1969 till 1993. He has been with the University of Pardubice since 1994. He is interested in numerical methods, simulations, measurements, radar antennas and propagation.